Angle-Retaining Color Space for Color Data Visualization and Analysis

Marco Buzzelli [1,*], Simone Bianco [1] and Raimondo Schettini [1]

[1] University of Milano - Bicocca; marco.buzzelli@unimib.it, simone.bianco@unimib.it, raimondo.schettini@unimib.it

***** Corresponding author: marco.buzzelli@unimib.it

Abstract

The Angle-Retaining Chromaticity diagram (ARC) is used to map tristimulus values in a two-dimensional representation, so that angular distances in the original three-dimensional space are preserved as Euclidean distances in ARC. This property makes the ARC diagram particularly useful for computational color constancy, where the illuminant intensity is purposely discarded and illuminant chromaticities are compared in terms of angular distances, through either the recovery error or the reproduction error. We expand the ARC diagram by designing a full-fledged color space that adopts a cylindrical-coordinate color model. The resulting ARC space incorporates a third dimension encoding the intensity information of the initial color, while maintaining the angle-retaining properties of the ARC diagram for the first two dimensions. We formalize the equations that describe the mutual conversion between RGB and ARC space. We illustrate the emerging geometric properties of the ARC space, and its relationship with angular distances. We present a number of potential applications of the ARC space related to color constancy, texture analysis, and image enhancement.

Keywords: *color constancy, illuminant estimation, white balance, chromaticity diagram, color space.*

INTRODUCTION

Computational color constancy, or "color constancy" for simplicity, aims at reducing the impact of the dominant illuminant source in a digital image. It is usually composed of two steps: the first one estimates the color of the scene illuminant by analyzing the image data, and the second one corrects the image itself by generating a new rendition of the scene, as if it was taken under a fixed reference light source. In order to evaluate the illuminant estimation part of computational color constancy, the error between a ground truth illuminant $U = (u_R, u_G, u_B)$ and an estimated illuminant $V = (v_R, v_G, v_B)$ is computed using the recovery angular error, which measures the three-dimensional angle in camera-raw RGB space between vectors U and V, thus ignoring their absolute intensity. Alternatively, Finlayson and Zakizadeh (2014) introduced the reproduction angular error as an alternative evaluation of color constancy algorithms, computing the angle between the "corrected" illuminant U/V and the neutral vector $(1,1,1)$.

In light of the relevance of angular distances for the field of color constancy, Buzzelli et al. (2020) designed an Angle-Retaining Chromaticity diagram (ARC) which maps, with a high level of accuracy, angular distances from the original RGB space into Euclidean distances on a plane. Here we further develop the chromaticity diagram by incorporating a third dimension which encodes the intensity information. The resulting three-dimensional color space fully characterizes the source data, while completely de-correlating the intensity information from the chromaticity information, and representing the latter in an angle-oriented interpretation that stems from the field of computational color constancy. As shown also in other fields of by Bianco et al. (2019), data representation can play a crucial role in successful computer vision, therefore we propose this alternative representation of color data with potential application to the fields of color constancy, texture analysis, enhancement, and in general all the applications in which intensity is processed independently from chrominance.

ORIGINAL TWO-DIMENSIONAL ARC DIAGRAM

Given an input RGB vector $P = (\rho_R, \rho_G, \rho_B)$, ARC polar coordinates $A = (\alpha_A, \alpha_R)$ (respectively hue-like and saturation-like) are computed as follows:

$$\alpha_A = \arctan2\left(\sqrt{3}(\rho_G - \rho_B), 2\rho_R - \rho_G - \rho_B\right), \tag{1}$$

$$\alpha_R = \arccos\left(\frac{\rho_R+\rho_G+\rho_B}{\sqrt{3}\sqrt{\rho_R^2+\rho_G^2+\rho_B^2}}\right). \tag{2}$$

Conversely, the inversion from ARC coordinates to RGB is described by the following relationship:

$$\begin{matrix}\frac{\rho_R}{\left|3\mathrm{sgn}(\alpha_A)\mathrm{sgn}(c)\sqrt{(c^2-c+1)d}+(c^2-c-2)d-(c^2-c+1)\right|} = \\ \frac{\rho_G}{|(c^2+2c+1)d-(c^2-c+1)|} = \\ \frac{\rho_B}{\left|3\mathrm{sgn}(\alpha_A)\sqrt{c^2(c^2-c+1)d}-(2c^2+c-1)d-(c^2-c+1)\right|},\end{matrix} \tag{3}$$

for brevity:

$$\frac{\rho_R}{k_R} = \frac{\rho_G}{k_G} = \frac{\rho_B}{k_B}. \tag{4}$$

This relationship describes a line in a three-dimensional space, obtained as the intersection between a cone and an half-plane, with both axes corresponding to the line of neutral grays in RGB space. The properties of such cone and half-plane relate to values c and d, computed from α_A and α_R as:

$$c = f_c(\alpha_A) = \frac{2\sqrt{3}}{\sqrt{3}-3\cot(\alpha_A)}, \tag{5}$$

$$d = f_d(\alpha_R) = \frac{\tan(\alpha_R)^2}{2}. \tag{6}$$

For numerical stability, the inversion Equation (3) is actualized in different ways, using either ρ_G or ρ_B as the independent variable.

THREE-DIMENSIONAL ARC SPACE

The introduction of the intensity component can be obtained in terms of distance between the initial RGB point and the point of origin (black):

$$\alpha_z = \sqrt{\rho_R^2 + \rho_G^2 + \rho_B^2}. \tag{7}$$

Assuming RGB values in the 0÷1 range, the α_z component will occupy the range between 0 and $\sqrt{3}$. In order to reconstruct the original RGB values from three-dimensional ARC values, we intersect the sphere defined by Equation (7) (having radius α_z and center in the origin) with the line in 3D space from (4). To do so, we solve Equation (4) for ρ_R and ρ_B:

$$\rho_R = \frac{k_R}{k_G}\rho_G, \tag{8}$$

$$\rho_B = \frac{k_B}{k_G}\rho_R, \tag{9}$$

and solve Equation (7) for the remaining variable ρ_G:

$$\rho_G = \sqrt{-\rho_R^2 - \rho_B^2 + \alpha_Z^2}. \tag{10}$$

By replacing the definition of ρ_B from Equation (9) into Equation (10), and subsequently replacing the resulting ρ_G in Equation (8), we make the value for ρ_R explicit. The same procedure can be applied to all variables:

$$\rho_R = \frac{k_R}{\sqrt{k_R^2+k_G^2+k_B^2}}\alpha_Z, \tag{11}$$

$$\rho_G = \frac{k_G}{\sqrt{k_R^2+k_G^2+k_B^2}}\alpha_Z, \tag{12}$$

$$\rho_B = \frac{k_B}{\sqrt{k_R^2+k_G^2+k_B^2}}\alpha_Z. \tag{13}$$

Note that in the original formulation from Buzzelli et al. (2020), the inversion led to a line in RGB space due to the lack of the intensity component. In this case, the inversion precisely leads to one point, so all variables are independently evaluated.

A special case is required when $\alpha_A = 0$, corresponding to the RGB plane of pure reds. In this case, we start from a set of simplified equations describing the line in three-dimensional space:

$$\rho_R = \rho_G \frac{2\sqrt{d}+1}{1-\sqrt{d}}, \tag{14}$$

$$\rho_B = \rho_G. \tag{15}$$

Adding to the procedure for the general case, we can substitute Equation (15) in Equation (10), thus obtaining:

$$\rho_R = \sqrt{\alpha_Z^2 - 2\rho_G^2}, \tag{16}$$

$$\rho_G = \frac{\sqrt{\alpha_Z^2-\rho_R^2}}{\sqrt{2}}. \tag{17}$$

Substituting either in Equation (14) eventually leads to:

$$\rho_R = \frac{\sqrt{\frac{4d+4\sqrt{d}+1}{2d+1}}}{\sqrt{3}}\alpha_Z, \tag{18}$$

$$\rho_G = \frac{\sqrt{\frac{d-2\sqrt{d}+1}{2d+1}}}{\sqrt{3}}\alpha_Z, \tag{19}$$

$$\rho_B = \rho_G = \frac{\sqrt{\frac{d-2\sqrt{d}+1}{2d+1}}}{\sqrt{3}}\alpha_Z. \tag{20}$$

An official implementation is made available at the project web page[1].

GEOMETRIC PROPERTIES OF ARC SPACE

The original ARC formulation is by design defined in polar coordinates (α_A, α_R), although the alternative Cartesian coordinates version (α_X, α_Y) also formulated by Buzzelli et al. (2020) is particularly useful when manipulating data in matrix form, and when computing Euclidean distances. By extension, the three-dimensional ARC space follows a cylindrical coordinate model, thus adhering to the same rationale of Hue-Saturation-* color spaces. The result of transforming the RGB cube gamut into ARC chromaticity and ARC color space is shown in Figure 1, with distances expressed in radians. The irregular shape of the three-dimensional solid on the right is a natural consequence of the intensity formulation expressed in Equation (7). The distance from the RGB origin is in fact different from the red green and blue group $(\alpha_Z = 1)$, for the cyan magenta and yellow group $\left(\alpha_Z = \sqrt{2}\right)$, and for the pure white $\left(\alpha_Z = \sqrt{3}\right)$.

[1] http://www.ivl.disco.unimib.it/activities/arc/

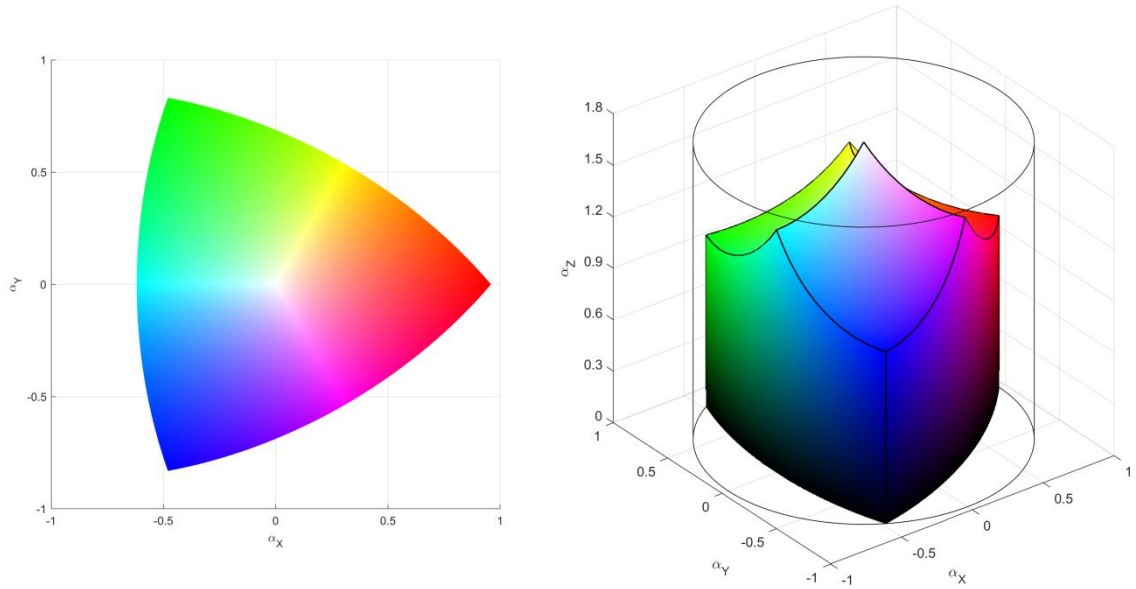

Figure 1: RGB gamut in Angle-Retaining Chromaticity diagram (left) and Angle-Retaining Color space (right).

Figure 2 offers a more clear visualization of the connection between RGB and ARC space: spheres of different radius having center in the RGB origin directly correspond to horizontal planes in ARC space, all having the same size. By design, then, rays emanating from the origin in RGB space, would map into parallel vertical lines in ARC space. Low-intensity RGB triplets get stretched out to span the same area of high-intensity ones, showing the connection with recovery angular error, according to which colors are compared by disregarding the intensity component. For the mere task of measuring color difference in ARC space, in fact, it is then sufficient to discard the newly-introduced α_Z value, and compute the Euclidean distance in the resulting two-dimensional space.

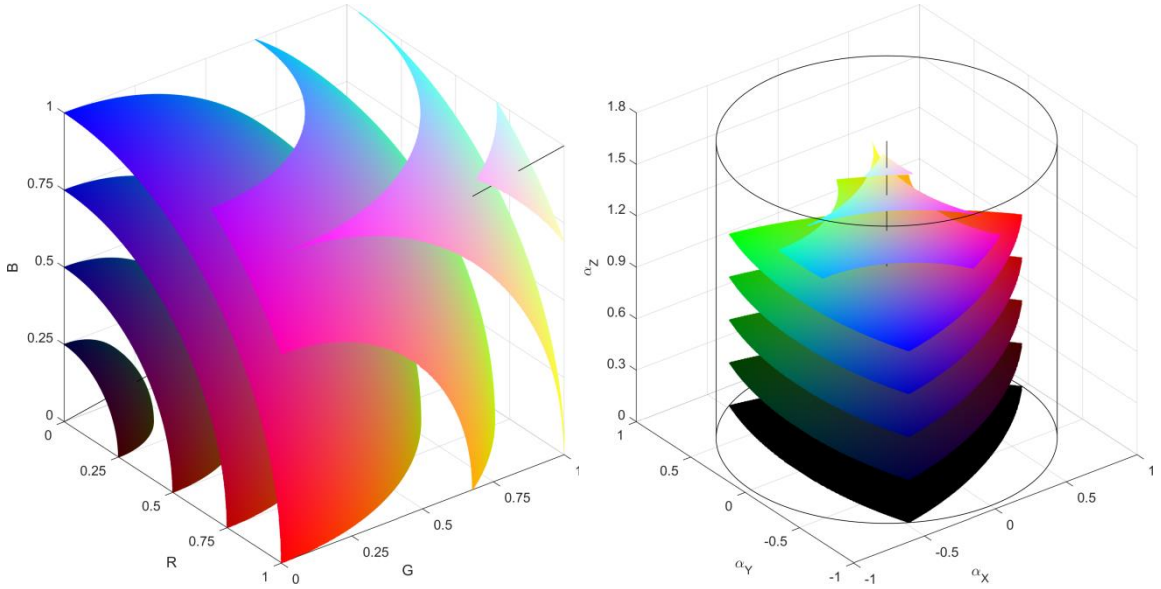

Figure 2: Concentric spheres in RGB space correspond to equal-sized horizontal parallel planes in ARC space.

POTENTIAL APPLICATIONS

Color constancy

The main application of two-dimensional and three-dimensional ARC is in the field of computational color constancy. In particular, the step of illuminant estimation takes as input an image in the RGB space of the specific camera (therefore, not sRGB nor any other device-independent space). This type of data is then manipulated and analyzed in order to produce an estimated RGB illuminant in the same camera-specific space, which is evaluated through the recovery and reproduction errors, both based on the assessment of angular distances. A full-fledged color space that encodes angular distances as Euclidean distances implicitly provides a sensitivity to the same angular distances that are used as target metric. As such, it could potentially facilitate an optimization process for illuminance estimation methods.

Texture analysis

Angle-based errors are also employed in the field of texture analysis. For example, Cusano et al. (2014) presented a feature for color texture classification, specifically designed to be robust against changes in the illumination conditions. Their descriptor combines a histogram of the Local Binary Patterns (LBPs) by Ojala et al. (1996), with a newly-introduced feature measuring the distribution of Local Color Contrast (LCC) based on the recovery angular error. Similarly, Li and Plataniotis (2018) introduced a compact rotation-invariant texture descriptor, named Quantized Diagnostic Counter-color Pattern (QDCP) for application in digital pathology image understanding. In a combination with Local Binary Patterns, they indexed local textons on the basis of color similarity quantified by the inner product of unit-length color vectors. Both works show that the inclusion of color-aware descriptors allows to outperform the original LBP approach, its color variants, as well as several other color texture descriptors in the state of the art, in classifying images acquired under varying illuminants. This suggests that other descriptors could be effortlessly enhanced with color-invariant properties by shifting to an ARC-based representation.

Finlayson et al. (1996) presented a color-based algorithm for recognizing colorful objects and textures, which relies on color distribution angles to index and retrieve such items. This type of application suggests the possibility of extending the angular color characterization to analyze the global distribution of an image.

Image denoising and enhancement

The separation of image data into color-related and intensity-related components has been successfully applied for applications of image denoising and, more generally, image enhancement. For example, Tang et al. (2001) introduced an algorithm that decomposes the input RGB into chromaticity and brightness, and then processes each component with a distinct approach. In particular, the chromaticity is transformed using a system of coupled diffusion equations adapted from the theory of harmonic maps in liquid crystals, while the brightness is enhanced by either a scalar median filter or an anisotropic diffusion flow. The impact of such decomposition-based approaches to image enhancement might benefit from the transition to ARC space in applications where the illuminant characterization should be preserved or treated in a special way.

Confirming the value of application to image enhancement, Vazquez-Corral and Bertalmio (2017) proposed a color-sensitive image decomposition to be applied before a typical denoising step. This decomposition produces multiple images in a spherical coordinate system, sharing some

commonalities with the proposed cylindrical ARC space, each having origin in a different color value, defined so as to be far away from the image dominant colors. They experimentally showed that this approach outperforms the results of directly applying different state-of-the-art denoising methods.

CONCLUSIONS

We have presented ARC: a new color space based on a cylindrical model that separates intensity, hue-like and saturation-like components, these last two specifically designed to map RGB angular distances into Euclidean distances. We have provided the mathematical formulation for both RGB-to-ARC and ARC-to-RGB conversion, illustrated the geometric properties of the resulting space, as well as its potential application to color constancy, texture analysis, and image enhancement.

As future development, the fields of hyperspectral and multispectral imaging could be investigated as a further case of application of angle-based analysis and representation.

REFERENCES

Bianco, S., M. Buzzelli, and R. Schettini. 2019. A unifying representation for pixel-precise distance estimation. *Multimedia Tools and Applications, 78*(10): 13767-13786.

Buzzelli, M., S. Bianco, and R. Schettini. 2020. ARC: Angle-Retaining Chromaticity diagram for color constancy error analysis. *JOSA A, 37*(11): 1721-1730.

Cusano, C., P. Napoletano, and R. Schettini. 2014. Combining local binary patterns and local color contrast for texture classification under varying illumination. *JOSA A, 31*(7): 1453-1461.

Finlayson, G. D., S. Chatterjee, and B. V. Funt. 1996. Color angular indexing. In: *European Conference on Computer Vision*, Springer, Berlin, Heidelberg, 16-27.

Finlayson, G. D., and R. Zakizadeh. 2014. Reproduction angular error: An improved performance metric for illuminant estimation. *Perception, 310*(1): 1-26.

Li, X., and K. N. Plataniotis. 2018. Novel chromaticity similarity based color texture descriptor for digital pathology image analysis. *Plos one, 13*(11): e0206996.

Ojala, T., M. Pietikäinen, and D. Harwood. 1996. A comparative study of texture measures with classification based on featured distributions. *Pattern recognition, 29*(1): 51-59.

Tang, B., G. Sapiro, V. and Caselles. 2001. Color image enhancement via chromaticity diffusion. *IEEE Transactions on Image Processing, 10*(5): 701-707.

Vazquez-Corral, J., and M. Bertalmio. 2017. Angular-based preprocessing for image denoising. *IEEE Signal Processing Letters, 25*(2): 219-223.